

Published in final edited form as:

Invest Ophthalmol Vis Sci. 2006 May ; 47(5): 2150–2160.

Characterization of Peripherin/*rds* and Rom-1 Transport in Rod Photoreceptors of Transgenic and Knockout Animals

Edwin S. Lee^{1,3}, Beth Burnside^{1,3}, and John G. Flannery^{2,3}

¹ Department of Molecular Cell Biology, University of California, Berkeley, Berkeley, California

² Department of Vision Science, University of California, Berkeley, Berkeley, California

³ Helen Wills Neuroscience Institute, University of California, Berkeley, Berkeley, California

Abstract

Purpose— Peripherin/*rds* and rom-1 have structural roles in morphogenesis and stabilization of the outer segment, but little is known about their transport and sorting to the rod outer segment. Peripherin/*rds* and rom-1 trafficking were studied in several knockout and transgenic animal models.

Methods— Rod outer segment formation and distribution of peripherin/*rds* and rom-1 were examined by immunohistochemistry, electron microscopy, and molecular biological methods in wild-type, rhodopsin-knockout, and peripherin/*rds*-knockout mice. C-terminally truncated peripherin/*rds* (Xper38)-GFP chimeric protein sorting was followed by immunofluorescence microscopy in transgenic *Xenopus*.

Results— In developing wild-type photoreceptors, peripherin/*rds* was detected exclusively in the distal tip of the connecting cilium in advance of outer segment formation. Rhodopsin-knockout mice failed to create normal rod outer segments and instead, elaborated membranous protrusions at the distal cilium tip. Peripherin/*rds* and rom-1 localized to this ciliary membrane in rhodopsinless photoreceptors. In transgenic *Xenopus*, a C-terminally truncated peripherin/*rds*-GFP fusion predominantly localized to its normal location within disc rims. In developing *rds* mice, rom-1 accumulated primarily in distal ciliary membranes.

Conclusions— Peripherin/*rds* transport and localization are polarized to the site of outer segment morphogenesis before disc formation in developing photoreceptors. Peripherin/*rds* and rom-1 trafficking is maintained in rhodopsin-knockouts, suggesting that rim proteins and rhodopsin have separate transport pathways. The presence of truncated peripherin/*rds*-GFP in the outer segment supports previous evidence that peripherin/*rds* mice form homotetramers for outer segment targeting. The finding that rom-1 transports to the outer segment domain in *rds* mice suggests that rom-1 may possess its own sorting and transport signals.

During rod photoreceptor development, a connecting cilium composed of a ring of nine microtubule doublets emerges from the inner segment, a specialized region that houses the photoreceptor's metabolic and biosynthetic machinery. Membranes and proteins amass at the tip of the cilium and eventually organize to form a highly ordered outer segment structure consisting of stacked discs ensheathed by an overlying plasma membrane. Rhodopsin, peripherin/*rds*, and rom-1 are integral membrane proteins that incorporate into newly forming discs, although peripherin/*rds* and rom-1 localize and function in a region distinct from rhodopsin. The light-sensing pigment, rhodopsin, resides in the lateral membrane of the disc

Corresponding author: John G. Flannery, Helen Wills Neuroscience, 112 Barker Hall University of California, Berkeley, Berkeley, CA; flannery@socrates.berkeley.edu.

Disclosure: **E.S. Lee**, None; **B. Burnside**, None; **J.G. Flannery**, None

Supported by Grants EY013533 and EY03575 from the National Eye Institute and by the Foundation Fighting Blindness.

face, whereas peripherin/*rds*, rom-1, and the flippase ABCR, are sorted and incorporated into disc rims.^{1–5} The precise mechanism controlling the partitioning of these molecules into separate regions of the disc remains unknown, although various studies have elucidated several aspects of rhodopsin trafficking from the Golgi to inner segment membranes and to the outer segment.⁶ Transport of other disc proteins such as peripherin/*rds* and rom-1 has been less well characterized even though they play important roles in the development and stability of the outer segment.

Peripherin/*rds* and rom-1 are *tetra*-spanning membrane proteins possessing a short cytoplasmic N terminus, an inner D2 loop, and a cytoplasmic C-terminal tail.^{2,7} The D2 loop is the site of noncovalent interactions between peripherin/*rds* and rom-1 heterotetramers.⁸ Both rim proteins are also capable of forming homotetramers, and peripherin/*rds* has been found to exist as higher order oligomeric complexes in the outer segment.^{8,9} Although rom-1 and peripherin/*rds* are structurally similar, they share only 30% identical sequences, mainly in the D2 loop.² Other differences include glycosylation of peripherin/*rds* and its twofold higher concentration than rom-1 in photoreceptor outer segments.⁹

Normal levels of peripherin/*rds* expression are necessary for the morphogenesis and maintenance of photoreceptor outer segments. Homozygous peripherin/*rds*-knockout mice that do not synthesize peripherin/*rds* fail to form outer segments and also undergo a slow degeneration, mirroring the phenotype of rhodopsin null mice.^{10–14} Even removal of one copy of peripherin/*rds* leads to genetic haploinsufficiency; characterized by the formation of disorganized outer segment membrane “whorls” in place of the rod outer segment, moderate rate of apoptotic photoreceptor cell death, and reduction in the electroretinogram (ERG) responses.¹⁵ Loss of rom-1 causes discs to become subtly disorganized and slightly shortened.¹⁶ Based on this result, the role of rom-1 is thought to add stability to outer segment discs, fine tuning its ultrastructure. It has also been suggested to play an accessory role in peripherin/*rds* mediated membrane fusion.¹⁷

Peripherin/*rds* mutations cause a variety of retinal abnormalities in affected individuals.¹⁸ Two premature stop mutations, Tyr258ter and Trp316ter, have been implicated in causing adult vitelliform macular dystrophies in humans, which are characterized by gradual photoreceptor degeneration and macroscopic retinal pigment epithelium (RPE) changes.^{19,20} Because a recent report has shown an outer segment targeting signal is located within residues 317 to 336 of *Xenopus* peripherin/*rds*,²¹ both Tyr258ter and Trp316ter mutations are predicted to generate C-terminally truncated peripherin/*rds* that is missing this transport signal. Whether the deletion affects localization of truncated peripherin/*rds* and how the loss of these residues promotes the disease phenotype has yet to be determined.

An earlier study of peripherin/*rds* and rhodopsin localization in detached feline retinas has provided some clues about the transport of peripherin/*rds*. After the retina was separated from the RPE, peripherin/*rds* was detectable only in the cytoplasm close to the striated rootlet, whereas rhodopsin delocalized to plasma membranes throughout the photoreceptor.²² The authors suggest that the distinct localization pattern is evidence of separate transport pathways. However, rim proteins may still depend on rhodopsin for transit to the outer segment, as the sheer abundance of rhodopsin transporting to the outer segment could facilitate the movement of other molecules such as rom-1 and peripherin/*rds* by providing material flux (i.e., bulk transport) or dominant transport signals. In mammalian photoreceptors, approximately 2000 rhodopsin molecules within 0.1 μm^2 of membrane passes through the connecting cilium per minute,²³ and rim proteins may transport passively along this gradient. Therefore, we sought to determine unequivocally whether the transport of rim proteins and rhodopsin are interdependent by examining peripherin/*rds* and rom-1 trafficking in rhodopsinless rods.

Very few studies have explored the transport of rom-1 in rod photoreceptors. Because its protein topology and localization to disc rims are essentially identical with peripherin/*rds*, one might expect rom-1 to interact with the same transport partners. However, the cytoplasmic C-terminal tail of rom-1 and peripherin/*rds* share only a small number of identical residues and may not share a common transport signal motif.^{2,24} In a recent study, a fusion protein composed of the C terminus of bovine rom-1 and green fluorescent protein (GFP) was unable to target normally to the outer segments in transgenic *Xenopus* photoreceptors, suggesting that rom-1 may not possess any transport signals in its C-terminal tail.²¹ Rom-1, however, is not normally expressed in *Xenopus* photoreceptors, making this result difficult to interpret.

To improve our understanding of the transport mechanism(s) of the disc rim proteins, peripherin/*rds* and rom-1, we have taken various approaches using wild-type, knockout, and transgenic animals. First, the normal localization of peripherin/*rds* was examined in developing rod photoreceptors, using wild-type rats. Next, rhodopsin-knockout mice were used to determine whether peripherin/*rds* and rom-1 are dependent on rhodopsin for transport to the outer segment membrane domain. We also generated transgenic *Xenopus* to study how the removal of a C-terminal transport signal from peripherin/*rds* would affect its targeting to outer segment disc rims. Finally, we examined *rds* mice to investigate whether rom-1 localizes properly in the absence of peripherin/*rds*.

Methods

Animals

All animals were treated in accordance with both the ARVO Statement for the Use of Animals in Ophthalmic and Vision Research and procedures approved by the University of California Animal Care and Use Committee.

Immunoelectron Microscopy

Retinas of wild-type rats (postnatal day [P]5, P6, P8, and P15) were carefully isolated, to minimize any tissue damage, and were fixed in buffered 4% paraformaldehyde and 0.5% glutaraldehyde for 2 hours. Buffer washes, ethanol dehydration steps, and incubation in lowicryl resin (K11M; Polysciences, Inc., Warrington, PA) were completed at progressively lower temperatures using a low-temperature embedding apparatus (Baltec; LTE 020; Furstentum, Liechtenstein). Resin was polymerized by illumination with UV light and 1 μ m sections for light microscopy were cut with an ultramicrotome (Leica, Deerfield, IL). Ultrathin (~70 nm) sections for transmission electron microscopy were placed on formvar-coated nickel grids and immunostained with either the anti-peripherin/*rds* antibody Per3B6 (1:200) or the anti-rhodopsin antibody Rho4D2 (1:100; gift of Robert Molday, University of British Columbia, Vancouver, Canada) followed by 5 to 10 nm gold-conjugated secondary antibodies (1:200; Ted Pella, Redding, CA). Sections were postfixated with 0.5% glutaraldehyde and counterstained with 2% uranyl acetate and 0.5% lead citrate. Images were viewed and captured with a JEOL 100CX electron microscope (JEOL USA, Peabody, MA). This procedure was repeated for P30 wild-type and P9, P30 rhodopsin-knockout mice using anti-peripherin/*rds*, Mper5H2 (1:10; gift of Robert Molday), or anti-rom-1 C-1 (acidic; 1:800; gift of Roderick McInnes, University of Toronto, Ontario, Canada). A minimum of two animals were used for each animal-antibody combination.

Scanning Electron Microscopy

The rhodopsin-knockout mice were kindly provided by Janis Lem (Tufts New England Medical Center, Boston, MA). Retinas from P7, P30, and P45 rhodopsin-knockout mice were isolated and fixed in 2% glutaraldehyde buffered in 0.1 M sodium cacodylate for 1 hour, followed by postfixation in 1% osmium tetroxide and 0.1 M sodium cacodylate. After fixation, retinas were

rinsed with cacodylate buffer, dehydrated in a graded series of ethanol, and dried by critical-point dehydration. Samples were mounted onto stubs and sputter coated with an 18-nm-thick layer of gold palladium. Images were captured with a cold-field emission scanning electron microscope (S-5000; Hitachi, Tokyo, Japan). A minimum of two animals were imaged at each age.

Electron Microscopy

Retinas of rhodopsin-knockout mice (P7, P30, and P45) were isolated for fixation overnight in a solution of 2% paraformaldehyde, 2% glutaraldehyde, and phosphate buffered saline (PBS). After fixation, retinas were rinsed, incubated in 2% osmium tetroxide in PBS for 2 hours, dehydrated in a graded ethanol series, and embedded in Epon/Araldite resin for polymerization at 65°C overnight. Seventy-nanometer sections were cut and placed on formvar-coated copper grids. Sections were stained with 2% uranyl acetate and counterstained with 0.5% lead citrate to enhance contrast. A JEOL 100CX electron microscope operating at 120 kV was used to image sections. At least two animals per age were prepared and imaged.

Quantitative Real-Time RT-PCR

Real-time RT-PCR was performed on P10 and P30 wild-type ($\rho^{+/+}$) and rhodopsin-knockout ($\rho^{-/-}$) animals. Retinas were homogenized (QiaSchredder columns; Qiagen, Valencia, CA), and RNA was isolated and purified (RNeasy kit; Qiagen). Equal amounts of RNA were treated with DNase I (Invitrogen, Carlsbad, CA) and reverse transcribed with an RT-PCR kit (Invitrogen) using the supplied oligo(dT) primers. The following gene-specific primers were designed (Vector NTI 9.0; Invitrogen): Rom-1 forward 5'-ATCCGTTTGGCACAGGGCAT-3' and reverse 5'-TAGAGCCACCGTTCCCGCTG-3'; Peripherin/*rds* forward 5'-GATCTGCTATGATGCCCTGGACC-3' and reverse 5'-TCAATCTGGAGCATGTTCGATGGT-3'; Thy-1 forward 5'-CGCGTACCCTCTCCAACCA-3' and reverse 5'-AACCAGCAGGCTTATGCCGC-3'. Twenty-five-microliter PCR reactions consisting of primers, cDNA, and master mix (SYBR Green; Applied Biosystems [ABI], Foster City, CA) were performed in a real-time detection system (MX3000P; Stratagene, La Jolla, CA) using the manufacturer's settings. The cycling parameters were as follows: denaturation, 94°C, 30 seconds; annealing 63°C, 30 seconds; extension 72°C, 30 seconds. Expression levels of peripherin/*rds* and rom-1 of one P30 wild-type animal (calibrator) were arbitrarily set to 100% and the relative expression levels were calculated using the formula $2^{-\Delta\Delta C_T}$, where $\Delta\Delta C_T = \Delta C_T(\text{sample}) - \Delta C_T(\text{calibrator})$.²⁵ ΔC_T corresponds to the difference in threshold cycles between the target gene (peripherin/*rds* or rom-1) and the reference, Thy-1. Measurements were taken from three animals per genotype per age.

Construct Generation

The construct for transgenic *Xenopus laevis* expression, XOP-peripherin/*rds* (XRDS 38)-GFP (a generous gift from Robert Molday) was designed in part by Chris Loewen (University of British Columbia). The plasmid was derived from peGFP-N1 by replacement of the CMV promoter with a fragment of the *Xenopus* opsin promoter (XOP)²⁶ and subcloning of full-length peripherin/*rds*-GFP into the *XhoI* and *NotI* sites of XOP1.3-eGFP-N1.²⁷ The C-terminal truncation construct, XOP-288-GFP, was generated from the parent plasmid by subcloning into *XhoI* and *EcoRI* sites, replacing the full-length peripherin/*rds* with the 864 bp (288 amino acid) truncated form. PCR products and constructs were sequenced to verify the correct modifications were made.

Xenopus Transgenics

Transgenesis consisted of sperm nuclear transplantation, as modified in prior studies.^{28,29} In brief, sperm nuclei were isolated from testes of an adult *Xenopus* injected with 300 U human chorionic gonadotropin (HCG; Fujisawa, USA, Inc., Elmsford, NY). The homogenized and pelleted sperm nuclei were detergent treated with NP-40 for membrane permeabilization before eventual resuspension in a glycerol–nuclear preparation buffer. Heated cytoplasmic egg extract was prepared and mixed with sperm nuclei and linearized plasmid DNA before injection into unfertilized eggs. Two to 5 nL of sperm nuclei–linearized DNA mix per egg was injected using a procedure described by Kroll and Amaya.²⁹ Eggs were placed at 15°C for 3 to 4 hours and properly dividing embryos were incubated at room temperature in 0.1 × Gerhart’s Ringer solution. At 5 to 6 days after fertilization, stage 40 to 42 tadpoles (see Nieuwkoop and Farber³⁰) were screened for retinal GFP expression with a fluorescence-equipped dissecting microscope.

Immunohistochemistry

Eyes were enucleated from P30 rhodopsin-knockout and wild-type mice, and the corneas were pierced with a surgical blade tip and immersed in 4% formaldehyde in PBS buffer for 5 to 10 minutes. P23 *rds* mice (kindly provided by Muna Naash; University of Oklahoma, Oklahoma City, OK) were prepared in a similar manner with 4% paraformaldehyde and overnight incubation. The cornea and lens were then removed and fixation continued for 1 hour. Eye cups were washed three times in PBS and cryoprotected with 15% sucrose for 2 hours, followed by overnight immersion in 30% sucrose. Specimens were embedded in OCT medium (Sakura Finetek USA, Torrance, CA) and frozen in a dry ice-ethanol bath. Seven- to 15-micrometer frozen sections were cut (Cryostat; Leica) and placed on glass slides. Tissue sections were blocked with 2% BSA, 0.1% FBS, and 1% Triton-X-100. Sections from rhodopsin-knockout and wild-type mice were co-immunostained with 1:800 anti-rom-1 C-1 (acidic), 1:15 anti-peripherin/*rds* Mper5H2 primary antibodies, and 1:1500 Cy3, 1:500 FITC-conjugated secondary antibodies. Sections from *rds* mice were incubated with 1:800 anti-rom-1 C-1 (acidic), 1:100 anti-rhodopsin, Rho4D2, and 1:1500 Cy3, 1:500 FITC conjugated secondary antibodies. Cryosections were counterstained with Hoechst 33342 dye (1:10,000; Invitrogen, Inc., Eugene, OR) for 1 minute before addition of antifade medium (Prolong; Invitrogen) to reduce bleaching. Labeling was performed on at least two mice.

For immunofluorescence microscopy of transgenic *Xenopus*, stage-48 to -53 frogs were first anesthetized with 0.028% benzocaine. Eyes were excised, fixed briefly in methanol or 4% paraformaldehyde, and either punctured carefully with a fine glass needle or cut, to remove the cornea. Eye cups were reimmersed in fixative overnight, placed in a graded series of sucrose solutions, embedded in OCT medium, and snap frozen in liquid nitrogen. Six- to 12-micrometer sections were prepared for imaging for GFP emission with an inverted fluorescence microscope (Axiophot; Carl Zeiss, Thornwood, NY).

Results

Rhodopsin and Peripherin/*rds* Localization in Developing Photoreceptors

We examined the transport of peripherin/*rds* and its involvement in outer segment formation in rat photoreceptors by immunocytochemistry, using Per3B6, a sensitive and specific antibody recognizing rat peripherin/*rds*. In our hands, the Per3B6 antibody was a more sensitive antibody for immunoelectron histochemical labeling of ultrathin sections than were antibodies against mouse peripherin/*rds*. At P5, the connecting cilium had formed, but disc membranes had not yet emerged from the distal tip of the cilia. Peripherin/*rds* was detected in a fraction of wild-type photoreceptors with the Per3B6 antibody and localized specifically to the distal connecting cilium at this age (Fig. 1A). At P6, increased levels of peripherin/*rds* was concentrated in the

distal connecting cilium, concomitant with the initial accumulation of membranes in this region (Fig. 1B). At P8, rod photoreceptors had formed disorganized, immature outer segments composed of unaligned and aligning discs (Fig. 1C). Anti-peripherin/*rds* labeling revealed varying amounts of peripherin/*rds* distributed throughout the outer segment membranes. By P15, stacked discs were observed in an ordered arrangement within outer segments, and peripherin/*rds* localized to disc rims (Fig. 1D). The inner segments (IS) of rat photoreceptors showed no peripherin/*rds* labeling at any age, when examined by immunoelectron microscopy. Figure 1E shows a P5 inner segment with no apparent membrane labeling. In contrast, rhodopsin was often detected in apical and lateral inner segment membranes of P5 photoreceptors (Fig. 1F). Rhodopsin was also present in the distal connecting cilium of P4 to P5 rats, and accumulated in the developing outer segments and inner segment plasma membrane at P7 to P8.^{31,32} By P15, rhodopsin was localized exclusively to the outer segments and was no longer detectable in the inner segment (data not shown).

Morphology of Rod Photoreceptors in Rhodopsin-Knockout Mice

To determine whether outer segment rim proteins rely on rhodopsin trafficking for transport from their site of synthesis in the inner segment to the outer segment, we followed rom-1 and peripherin/*rds* localization in photoreceptors of rhodopsin-knockout mice.¹³ Before initiating the localization studies, we assessed the ultrastructure of rhodopsin-knockout mice retinas, specifically looking for formation of outer segment membranes in the region of the distal connecting cilium. It has been noted that elongated outer segments do not form in these animals when imaged at the light microscopic level.^{13,14} However, photoreceptor morphology of rhodopsin-knockout mice has not been thoroughly examined. Scanning electron microscopy (SEM) was performed for high resolution imaging of the inner and outer segment landscape (Figs. 2A–E). At P7, photoreceptors of rhodopsin-knockout mice created a bare connecting cilium, devoid of membrane accumulation at the distal tip (Fig. 2A)—a morphology similar in appearance to rod photoreceptors of the *rds* mice with a null mutation in the peripherin/*rds* gene and characterized by abnormal outer segments.^{11,12} Photoreceptors of P7 wild-type mice and rats normally create small, rudimentary outer segment membranes at the tip of the connecting cilium.^{31,33,34} By P30, long, cylindrical outer segments were observed in wild-type photoreceptors (Fig. 2B). In contrast, most P30 photoreceptors of the rhodopsin-knockout (*rho*^{-/-}) mice formed small membrane sacs emerging from the distal connecting cilium (Fig. 2C). These outer segment domain (OSD) membranes often appeared as thin tubes tapering at the proximal and distal ends. On occasion, membrane “towers” were observed budding from the inner segment in P30 rhodopsin-knockout photoreceptors (Fig. 2D). In P45 rods, the volume of accumulated membranes varied dramatically, as a small percentage of photoreceptors retaining their outer segment membranes were interspersed among photoreceptors with bare or absent connecting cilia (Fig. 2E).

Cross-sections of rhodopsin-knockout photoreceptors were imaged by transmission electron microscopy to examine the morphology of the outer segment domain membranes. By P7, the connecting cilium had developed normally, but lacked any accumulation of membranes inside the distal ciliary membrane (Fig. 2F). At P30, the ciliary tip membrane had expanded and some internal membranes were seen (Fig. 2G). Higher magnification longitudinal cross sections showed an accumulation of membranes with tubular or vesicular profiles oriented in various directions, but ordered discs were never observed (Fig. 2H). By P45, a few (*rho*^{-/-}) photoreceptors had created larger outer segment domains (Fig. 2I) compared with P30, but most membranes had regressed in size. Occasionally, layers of membranes were seen accumulating around a dense core of material within the inner segments (Fig. 2K). In a small fraction of photoreceptors, we observed mislocalized membranes protruding from the apical inner segment rather than associated with the connecting cilium. These membrane “towers” were also composed of tubular and vesicular elements (Fig. 2J) and their formation may

indicate a cell in a state of apoptosis. Protrusions from inner segment membranes have been observed in degenerating retinas and correlate with intermediate stages of apoptosis.^{35–38}

Transcription of *Peripherin/rds* and *Rom-1* Message in Rhodopsin-Knockout Photoreceptors

Transportation of vesicles carrying other outer segment proteins, such as the rim proteins, may contribute to distal accumulation of membranes in the absence of rhodopsin synthesis. To determine whether rhodopsin-knockout photoreceptors continue to synthesize rim proteins, we performed real-time RT-PCR (SYBR Green Master Mix; ABI) to quantify the expression levels of *peripherin/rds* and *rom-1* in rhodopsin-knockout retinas relative to wild-type. The levels of *peripherin/rds* and *rom-1* expression were normalized against the reference gene *Thy-1*, and results are displayed in Figure 3 as a percentage change relative to a P30 wild-type mouse (calibrator). *Peripherin/rds* was expressed at ~80% of aged-matched wild-type levels in P10 rhodopsin-knockout mice, and ~70% of wild-type levels at P30 (Fig. 3A). Relative to age-matched control mice, rhodopsin-knockout mice expressed *rom-1* at ~70% levels in P10 mice, and ~60% of wild-type levels in older P30 mice (Fig. 3B). Collectively, these data indicate that expression of rim proteins in rhodopsin-knockout photoreceptors is reduced, but remains relatively robust. Of note, retinas of older (P30) wild-type and knockout animals had higher expression levels of *peripherin/rds* relative to developing P10 retinas (Fig. 3A), whereas *rom-1* transcript levels showed little if any change between the two ages (Fig. 3B).

Localization of Outer Segment Rim Proteins in Rhodopsin-Knockout Mice

Using both fluorescence and electron microscopy, we examined the localization of *rom-1* and *peripherin/rds* in retinas from P30 rhodopsin-knockout animals. At this age, accumulation of outer segment domain membranes is prominent and photoreceptor degeneration is minimal. Immunohistochemistry was performed on 7- to 10- μ m frozen sections from a minimum of two rhodopsin-knockout mice. By fluorescence microscopy, *peripherin/rds* was observed to localize prominently in the outer segment region, with virtually no signal present in the inner segment, except for an occasional photoreceptor (Fig. 4A). *Rom-1* colocalized with *peripherin/rds* in outer segment domain membranes and was mostly absent from inner segments and the outer nuclear layer (Figs. 4B, 4C). Rarely, a cell was observed with *rom-1* delocalization to the cell body, possibly signifying a dying cell (Fig. 4B). Rhodopsin-knockout retinal sections did not stain with rhodopsin antibodies, and only nonspecific RPE background and OS autofluorescence was detected (Fig. 4D). In control wild-type mice, anti-*peripherin/rds*, anti-*rom-1*, and anti-rhodopsin antibody labeling was restricted to outer segment membranes (Figs. 4E–H).

Immunoelectron microscopy was performed to visualize the pattern of *rom-1* localization in developing and adult rhodopsin-knockout photoreceptors. Anti-*rom-1* C-1 antibody specifically labeled *rom-1* in the disc rims of wild-type P30 rod photoreceptors (Fig. 4I). In immature P7 rhodopsin-knockout photoreceptors, low amounts of *rom-1* was detectable in the distal connecting cilium, but no label was found in the inner segments (Fig. 4J). By P30, large concentrations of *rom-1* had accumulated in the expanding outer segment domain membranes, amassing distal to the connecting cilium (Fig. 4K). Rhodopsin-knockout photoreceptors labeled with *peripherin/rds* Mper5H2 antibodies exhibited the same localization pattern as *rom-1*—that is, labeling was present in the outer segment and absent from the inner segment (Fig. 4L). In a few cells possessing abnormal whorls of membranes in the inner segment, *rom-1* was observed to colocalize with the ectopic inner segment membrane accumulations (Fig. 4M). Taken together, the results of our immunohistochemistry experiments demonstrate that rim protein transport to the outer segment domain is independent of rhodopsin translocation.

Expression of C-terminally Truncated Peripherin/*rds*-GFP in Transgenic *Xenopus* Photoreceptors

Mutations in peripherin/*rds* that delete portions of the C-terminal tail has been implicated in causing retinal disease.^{18,20} Recently, the C terminus of peripherin/*rds* was found to mediate outer segment transport,²¹ but it is not known how its removal affects trafficking. To have a better understanding of the trafficking and disease pathogenesis of truncated peripherin/*rds* mutations, we created transgenic *Xenopus* that expressed a C-terminally truncated peripherin/*rds* attached to GFP (Xper288) under the control of an opsin promoter. Transgenic *Xenopus* expressing full-length peripherin/*rds* fused with GFP (Xper346) were also generated. Figures 5A and 5B show the fusion proteins synthesized. Transgene expression was restricted to photoreceptors and displayed a slight mosaic pattern throughout the retina (Fig. 5C). Variation within a cell, between photoreceptors in the retina and from one animal to another has been documented in transgenic *Xenopus*.^{21,27,28,39,40} This variation is thought to be attributable to random transgene silencing from position-effect variegation.⁴¹ In photoreceptors, C-terminally truncated peripherin/*rds*-GFP (Xper288) predominantly localized to outer segments, often specifically in disc rims and incisures despite missing its C-terminal tail (Figs. 5D, 5F). The localization of Xper288 in incisures appeared as vertical striations in the outer segments (Figs. 5D, 5F) as well as scalloped pattern in transverse sections (Fig 5H). Occasionally, the Xper288 fusion protein was also observed at low densities within the inner segment (Fig. 5F). Control full-length peripherin/*rds*-GFP (Xper346) localized normally to the disc rims and incisures of photoreceptors expressing moderate quantities of the fusion protein (Figs. 5G, 5I), indicating that the fusion of GFP to the C-terminal tail does not significantly alter its transport and incorporation into disc rims. The outer segment morphology in Xper288 mutant and Xper346 photoreceptors appeared normal, although occasional incisures may have been slightly disorganized, based on the aberrant fusion protein localization within the outer segment. Protein missorting within the outer segment and constriction in high expressing photoreceptors were observed in transgenic *Xenopus* expressing full-length peripherin/*rds*-GFP.⁴⁰ Retinal degeneration was not evident in young Xper288 or control Xper346 transgenic tadpoles 14 to 15 days after fertilization. In a few photoreceptors expressing high levels of Xper346, an accumulation of the peripherin/*rds* fusion protein was also observed as a thick vertical column in the outer segment of longitudinal sections, and as a focal concentration in transverse cross sections (Fig. 5J). The observation that peripherin/*rds* fusion protein lacking its C-terminal transport signal can target correctly to disc rims, coupled with the finding that only an occasional photoreceptor exhibits low levels of delocalized peripherin/*rds*, suggests that the disease phenotype of patients with peripherin/*rds* truncation mutations is not caused by mislocalization. These results also suggest that the C terminus is not necessary for transport in the presence of endogenous peripherin/*rds*.

Rom-1 and Rhodopsin Localization in *rds* Mice

Rom-1 and peripherin/*rds* have been shown to exist as heterotetramers in the outer segment.⁸ It has been suggested that rom-1 may not contain its own sorting signals and cotransports with peripherin/*rds* in post-Golgi vesicles as heterotetramers. To determine whether rom-1 trafficking is dependent on peripherin/*rds*, we observed the transport and localization of rom-1 in *rds* mice lacking peripherin/*rds*. Photoreceptors of *rds* mice are unable to construct a proper outer segment; however, they do amass membranes and proteins at the distal connecting cilium in a manner similar to rhodopsin-knockout mice.^{11,12,36,37} In frozen sections of P23 *rds* retinas, labeling of rom-1 was concentrated primarily in the putative outer segment domain regions and, to a lesser extent, in the inner segment, cell body, and synaptic terminal (Fig. 6A). This labeling pattern indicates that a substantial fraction of rom-1 can reach the distal connecting cilium and incorporate into the outer segment membrane in the absence of peripherin/*rds*. Rhodopsin distribution in *rds* photoreceptors was similar to that of rom-1, with high levels in the putative outer segment region and some delocalization to the inner segment,

cell body, and synaptic terminals (Fig. 6B). Rom-1 was observed to colocalize with rhodopsin in *rds* retinas (Fig. 6C).

Discussion

The data presented in this study have provided further insights into the trafficking mechanisms of two integral rim proteins: peripherin/*rds* and rom-1. We have shown that in rat photoreceptors, peripherin/*rds* transports and localizes to the distal connecting cilium as early as P5. To our knowledge, this is the earliest developmental age that peripherin/*rds* protein has been visualized in photoreceptors, although the mRNA of its major transcripts has been detected as early as P1.⁴² At P5, connecting cilia have formed, but outer segment membranes are generally absent at this early stage of photoreceptor development. The appearance of peripherin/*rds* in the membrane-bare distal connecting cilium indicates that rim proteins are delivered to the site of outer segment morphogenesis in advance of disc assembly. In addition, the presence of neighboring photoreceptors without peripherin/*rds* labeling suggests that the onset of rim protein expression is not entirely synchronized during early photoreceptor development.

The polarized distribution of peripherin/*rds* exclusively to the distal connecting cilium and outer segment domain during early development contrasts with rhodopsin distribution in both inner and outer segment membranes. It has been previously hypothesized that the transport machinery of rhodopsin may be immature and inefficient in directing high levels of rhodopsin at early developmental stages, thus leading to the observed delocalization to inner segment membranes.³¹ Though it is still a possibility that peripherin/*rds* is present in the inner segment at levels below detection by our assay, it is interesting that peripherin/*rds* has not been observed to accumulate heavily in the photoreceptor inner segment membranes of various wild-type, transgenic, and knockout animals. We did not observe peripherin/*rds* inner segment membrane localization in developing wild-type or rhodopsin-knockout photoreceptors. In addition, retinal detachment in cats only resulted in delocalization of peripherin/*rds* near the striated rootlet and in the cytoplasm, not in the plasma membrane as observed with rhodopsin.²² Moreover little if any mutant C214S peripherin/*rds*-GFP inner segment mislocalization was observed in the plasma membrane at the electron microscopic level.⁴⁰ Together, these observations are consistent with the interpretation that a mechanism may exist to restrict incorporation of peripherin/*rds* into apical and lateral inner segment membranes.²²

Using a knockout mouse strategy, we have demonstrated that integral disc proteins peripherin/*rds* and rom-1 are able to transport to the outer segment membrane domain independent of rhodopsin. Even in the complete absence of rhodopsin, peripherin/*rds* and rom-1 continued to be incorporated into the outer segment domain membranes at the distal end of the cilium. This finding strongly suggests that rim proteins and rhodopsin have separate transport pathways to the outer segment. Indeed, an outer segment targeting signal was identified recently in the C terminus of *Xenopus* peripherin/*rds*,²¹ although rom-1 targeting signals have not been elucidated. The transport signal sequence of rhodopsin is also contained in the C terminus, but does not share any obvious motifs with peripherin/*rds*. Therefore, these two disc proteins may interact with different partner molecules for transit to the OS and incorporation into disc membranes. This hypothesis is indirectly supported by observations that selective removal of kinesin II in mice photoreceptors disrupts rhodopsin trafficking but has no discernable effects on peripherin/*rds*, suggesting that kinesin II may mediate rhodopsin transport but not peripherin/*rds*.⁴³ Although kinesin II has not been shown to interact directly with rhodopsin, there is precedence that outer segment proteins can bind to motor proteins, as rhodopsin has been shown to interact with Tctex-1, a dynein light chain.⁴⁴ By analogy, peripherin/*rds* may interact with other motor proteins in the inner segment and/or within the connecting cilium for outer segment transport.

The trafficking mechanism of peripherin/*rds* was further examined in vivo with the creation of transgenic *Xenopus laevis* expressing a peripherin/*rds* truncation mutant. The removal of the C-terminal of a *Xenopus* peripherin/*rds* orthologue, Xper38, did not significantly affect its transport, since mutant peripherin/*rds* was still distributed to the disc rims in rod photoreceptors, and only an occasional photoreceptor accumulated low levels of mutant protein within the inner segment. This finding is in stark contrast to the substantial mislocalization of rhodopsin truncation mutants observed in transgenic animals^{27,45,46} and is somewhat unexpected in light of the aforementioned discovery that the C-terminal fragment of peripherin/*rds* contains an outer segment localization signal.²¹ It is possible that truncated peripherin/*rds* is cotransported along with endogenous peripherin/*rds* to the outer segment rims. Peripherin/*rds* molecules have been shown to interact both covalently and noncovalently via the large intra-discal D2 loops to form dimers, tetramers, and higher-order oligomers.^{8,9} In a recent work, peripherin/*rds* mutants unable to form stable tetramers do not pass a “transport checkpoint” for incorporation into outer segment discs and delocalize to the inner segment,⁴⁰ strongly suggesting that peripherin/*rds* are transported as tetramers and/or larger oligomers. A simple alternate hypothesis is that peripherin/*rds* has secondary transport signals not present in the C-terminal tail that compensate for the removal of the primary signal(s). Expression of C-terminally truncated peripherin/*rds* on a peripherin/*rds*-knockout background may help distinguish between these two possibilities.

Human carriers of the 258ter and 317ter peripherin/*rds* truncation mutations have a phenotype consisting of mild functional changes, RPE abnormalities, and slight degeneration.^{18,20} By analogy with truncated rhodopsin mutants, the C-terminal truncation of peripherin/*rds* may harm rod photoreceptors through mislocalization to the inner segment. However, our results suggest that adult vitelliform macular dystrophy linked with these mutations may not be caused by toxic build-up of mutant peripherin/*rds* in inner segment, as mislocalization was rarely detected, and degeneration was not observed. Another mutant, peripherin/*rds* (C214S), also failed to induce degeneration in transgenic *Xenopus* although a high concentration of mutant peripherin/*rds*-GFP delocalized to the inner segment.⁴⁰ It is still a possibility that photoreceptor cell loss initiates at a later time point and should be assessed in older animals. Of note, the C-terminal of peripherin/*rds* has also been shown to function as a fusogenic core, possibly facilitating the pinching off of disc packets during disc shedding and phagocytosis.⁴⁷ This process may be abnormal in rod outer segments containing a mixture of truncated and normal peripherin/*rds*, leading to the observed retinal changes.

Our study on rom-1 trafficking in rod photoreceptors lacking peripherin/*rds* has indicated that a substantial fraction of rom-1 can transport to the outer segment region in the absence of peripherin/*rds*. This result suggests that rom-1 contains its own transport signals, most likely residing in the C-terminal tail as characteristic of other outer segment proteins.^{21,26,48} A fraction of rom-1 exists as homotetramers in the outer segment and by analogy with peripherin/*rds*, may translocate in this form through the inner segment. Rom-1 may also complex with peripherin/*rds* as heterotetramers for targeting to the outer segment. Of note, rom-1 has been shown to exist in distinct lipid rafts devoid of peripherin/*rds* in normal outer segment discs.¹⁷ Rom-1 may sort independently from peripherin/*rds* via lipid rafts in the Golgi apparatus, where rafts have been shown to play roles in protein sorting.⁴⁹ In addition to OS localization, low to moderate amounts of rom-1 mislocalized to the inner segment, cell body and the synaptic terminal. We believe that the mislocalized rom-1 is a secondary affect of the lack of outer segment formation coupled with rhodopsin expression. According to this scenario, high levels of rhodopsin and rom-1 might accumulate rapidly in the confined space of the distal connecting cilium membranes, leaving inadequate room for incorporation of newly synthesized proteins. Consistent with this interpretation, high levels of rom-1 were able to incorporate into outer segment domain membranes of rhodopsin-knockout photoreceptors completely removed of

rhodopsin. This could probably be clarified by observing rom-1 transport in rhodopsin and peripherin/*rds* double-knockout mice.

The role of transport motifs in outer segment trafficking is not yet fully understood. In epithelial cells, motifs such as dileucine and tyrosine have been implicated, mainly hypothesized to play a role in endosomal transport.⁵⁰ Recently, outer segment localization signals were discovered in the C-terminal tail of retinal dehydrogenase, prompting the authors to suggest that a (V/I) XPX transport motif exists in photoreceptors.⁵¹ However, this motif is not found in ABCR, peripherin/*rds*, and rom-1, suggesting that multiple and degenerate signals are used to guide outer segment protein transport and disc assembly. Further studies are needed to elucidate the molecular mechanisms governing transport of outer segment proteins necessary for the morphogenesis, maintenance, and function of rod photoreceptors.

Acknowledgements

The authors thank Alexander Quiambao for technical assistance with *rds* mice; Jennifer Lin-Jones and Mike Wu for help generating transgenic *Xenopus*, and investigators in the Flannery Laboratory for useful comments on the manuscript.

References

1. Arikawa K, Molday LL, Molday RS, Williams DS. Localization of peripherin/*rds* in the disk membranes of cone and rod photoreceptors: relationship to disk membrane morphogenesis and retinal degeneration. *J Cell Biol* 1992;116:659–667. [PubMed: 1730772]
2. Bascom RA, Manara S, Collins L, Molday RS, Kalnins VI, McInnes RR. Cloning of the cDNA for a novel photoreceptor membrane protein (rom-1) identifies a disk rim protein family implicated in human retinopathies. *Neuron* 1992;8:1171–1184. [PubMed: 1610568]
3. Moritz OL, Molday RS. Molecular cloning, membrane topology, and localization of bovine rom-1 in rod and cone photoreceptor cells. *Invest Ophthalmol Vis Sci* 1996;37:352–362. [PubMed: 8603840]
4. Papermaster DS, Schneider BG, Zorn MA, Kraehenbuhl JP. Immunocytochemical localization of a large intrinsic membrane protein to the incisures and margins of frog rod outer segment disks. *J Cell Biol* 1978;78:415–425. [PubMed: 690173]
5. Illing M, Molday LL, Molday RS. The 220-kDa rim protein of retinal rod outer segments is a member of the ABC transporter superfamily. *J Biol Chem* 1997;272:10303–10310. [PubMed: 9092582]
6. Sung CH, Tai AW. Rhodopsin trafficking and its role in retinal dystrophies. *Int Rev Cytol* 2000;195:215–267. [PubMed: 10603577]
7. Connell GJ, Molday RS. Molecular cloning, primary structure, and orientation of the vertebrate photoreceptor cell protein peripherin in the rod outer segment disk membrane. *Biochemistry* 1990;29:4691–4698. [PubMed: 2372552]
8. Goldberg AF, Molday RS. Subunit composition of the peripherin/*rds*-rom-1 disk rim complex from rod photoreceptors: hydrodynamic evidence for a tetrameric quaternary structure. *Biochemistry* 1996;35:6144–6149. [PubMed: 8634257]
9. Loewen CJ, Molday RS. Disulfide-mediated oligomerization of Peripherin/Rds and Rom-1 in photoreceptor disk membranes: implications for photoreceptor outer segment morphogenesis and degeneration. *J Biol Chem* 2000;275:5370–5378. [PubMed: 10681511]
10. Sanyal S, De Ruiter A, Hawkins RK. Development and degeneration of retina in *rds* mutant mice: light microscopy. *J Comp Neurol* 1980;194:193–207. [PubMed: 7440795]
11. Sanyal S, Jansen HG. Absence of receptor outer segments in the retina of *rds* mutant mice. *Neurosci Lett* 1981;21:23–26. [PubMed: 7207866]
12. Jansen HG, Sanyal S. Development and degeneration of retina in *rds* mutant mice: electron microscopy. *J Comp Neurol* 1984;224:71–84. [PubMed: 6715580]
13. Lem J, Krasnoperova NV, Calvert PD, et al. Morphological, physiological, and biochemical changes in rhodopsin knockout mice. *Proc Natl Acad Sci USA* 1999;96:736–741. [PubMed: 9892703]
14. Humphries MM, Rancourt D, Farrar GJ, et al. Retinopathy induced in mice by targeted disruption of the rhodopsin gene. *Nat Genet* 1997;15:216–219. [PubMed: 9020854]

15. Cheng T, Peachy NS, Li S, et al. The effect of peripherin/rds haploinsufficiency on rod and cone photoreceptors. *J Neurosci* 1997;17:8118–8128. [PubMed: 9334387]
16. Clarke G, Goldberg AF, Vidgen D, Collins L, et al. Rom-1 is required for rod photoreceptor viability and the regulation of disk morphogenesis. *Nat Genet* 2000;25:67–73. [PubMed: 10802659]
17. Boesze-Battaglia K, Dispoto J, Kahoe MA. Association of a photoreceptor-specific tetraspanin protein, ROM-1, with triton X-100-resistant membrane rafts from rod outer segment disk membranes. *J Biol Chem* 2002;277:41843–41849. [PubMed: 12196538]
18. Kohl S, Giddings I, Besch D, Apfelstedt-Sylla E, Zrenner E, Wissinger B. The role of the peripherin/RDS gene in retinal dystrophies. *Acta Anat (Basel)* 1998;162:75–84. [PubMed: 9831753]
19. Wells J, Wroblewski J, Kenn J, Inglehearn C, et al. Mutations in the human retinal degeneration slow (RDS) gene can cause either retinitis pigmentosa or macular dystrophy. *Nat Genet* 1993;3:213–218. [PubMed: 8485576]
20. Felbor U, Schilling UH, Weber BH. Adult vitelliform macular dystrophy is frequently associated with mutations in the peripherin/RDS gene. *Hum Mutat* 1997;10:301–309. [PubMed: 9338584]
21. Tam BM, Moritz OL, Papermaster DS. The C terminus of peripherin/rds participates in rod outer segment targeting and alignment of disk incisures. *Mol Biol Cell* 2004;15:2027–2037. [PubMed: 14767063]
22. Fariss RN, Molday RS, Fisher SK, Matsumoto B. Evidence from normal and degenerating photoreceptors that two outer segment integral membrane proteins have separate transport pathways. *J Comp Neurol* 1997;387:148–156. [PubMed: 9331178]
23. Besharse, JC. Photosensitive membrane turnover: differentiated membrane domains and cell-cell interaction. In: Adler, R.; Farver, D., editors. *The Retina, a Model for Cell Biological Studies*. San Diego, CA: Academic Press; 1986. p. 297-352.
24. Kedziński W, Moghrabi WN, Allen AC, et al. Three homologs of rds/peripherin in *Xenopus laevis* photoreceptors that exhibit covalent and non-covalent interactions. *J Cell Sci* 1996;109:2551–2560. [PubMed: 8923216]
25. Pfaffl MW. A new mathematical model for relative quantification in real-time RT-PCR. *Nucleic Acids Res* 2001;29:2002–2007.
26. Batni S, Mani SS, Schlueter C, Ji M, Knox BE. *Xenopus* rod photoreceptor: model for expression of retinal genes. *Methods Enzymol* 2000;316:50–64. [PubMed: 10800668]
27. Tam BM, Moritz OL, Hurd LB, Papermaster DS. Identification of an outer segment targeting signal in the COOH terminus of rhodopsin using transgenic *Xenopus laevis*. *J Cell Biol* 2000;151:1369–1380. [PubMed: 11134067]
28. Lin-Jones J, Parker E, Wu M, Knox BE, Burnside B. Disruption of kinesin II function using a dominant negative-acting transgene in *Xenopus laevis* rods results in photoreceptor degeneration. *Invest Ophthalmol Vis Sci* 2003;44:3614–3621. [PubMed: 12882815]
29. Kroll KL, Amaya E. Transgenic *Xenopus* embryos from sperm nuclear transplantations reveal FGF signaling requirements during gastrulation. *Development* 1996;122:3173–183. [PubMed: 8898230]
30. Nieuwkoop, PD.; Farber, J., editors. *Normal Table of Xenopus laevis (Daudin): a Systematical and Chronological Survey of the Development from the Fertilized Egg Till the End of Metamorphosis*. New York: Garland Publishers; 1994.
31. Nir I, Cohen D, Papermaster DS. Immunocytochemical localization of opsin in the cell membrane of developing rat retinal photoreceptors. *J Cell Biol* 1984;98:1788–1795. [PubMed: 6233288]
32. Hicks D, Barnstable CJ. Lectin and antibody labelling of developing rat photoreceptor cells: an electron microscope immunocytochemical study. *J Neurocytol* 1986;15:219–230. [PubMed: 3755163]
33. Olney JW. An electron microscopic study of synapse formation, receptor outer segment development, and other aspects of developing mouse retina. *Invest Ophthalmol Vis Sci* 1968;7:250–268.
34. Galbavy ES, Olson MD. Morphogenesis of rod cells in the retina of the albino rat: a scanning electron microscopic study. *Anat Rec* 1979;195:707–717. [PubMed: 525833]
35. Blanks JC, Mullen RJ, LaVail MM. Retinal degeneration in the pcd cerebellar mutant mouse. II. Electron microscopic analysis. *J Comp Neurol* 1982;212:231–246. [PubMed: 7153375]

36. Jansen HG, Sanyal S, De Grip WJ, Schalken JJ. Development and degeneration of retina in rds mutant mice: ultraimmunohistochemical localization of opsin. *Exp Eye Res* 1987;44:347–361. [PubMed: 2954840]
37. Usukura J, Bok D. Changes in the localization and content of opsin during retinal development in the rds mutant mouse: immunocytochemistry and immunoassay. *Exp Eye Res* 1987;45:501–515. [PubMed: 2962880]
38. Liepins A, Bustamante JO. Cell injury and apoptosis. *Scanning Microsc* 1994;8:631–641. [PubMed: 7747162]
39. Moritz OL, Tam BM, Papermaster DS, Nakayama T. A functional rhodopsin-green fluorescent protein fusion protein localizes correctly in transgenic *Xenopus laevis* retinal rods and is expressed in a time-dependent pattern. *J Biol Chem* 2001;276:28242–28251. [PubMed: 11350960]
40. Loewen CJ, Moritz OL, Tam BM, Papermaster DS, Molday RS. The role of subunit assembly in peripherin-2 targeting to rod photoreceptor disk membranes and retinitis pigmentosa. *Mol Biol Cell* 2003;14:3400–3413. [PubMed: 12925772]
41. Karpen GH. Position-effect variegation and the new biology of heterochromatin. *Curr Opin Genet Dev* 1994;4:281–291. [PubMed: 8032206]
42. Cheng T, al Ubaidi MR, Naash MI. Structural and developmental analysis of the mouse peripherin/rds gene. *Somat Cell Mol Genet* 1997;23:165–183. [PubMed: 9330629]
43. Marszalek JR, Liu X, Roberts EA, Chui D, et al. Genetic evidence for selective transport of opsin and arrestin by kinesin-II in mammalian photoreceptors. *Cell* 2000;102:175–187. [PubMed: 10943838]
44. Tai AW, Chuang JZ, Bode C, Wolfrum U, Sung CH. Rhodopsin's carboxy-terminal cytoplasmic tail acts as a membrane receptor for cytoplasmic dynein by binding to the dynein light chain Tctex-1. *Cell* 1999;97:877–887. [PubMed: 10399916]
45. Green ES, Menz MD, LaVail MM, Flannery JG. Characterization of rhodopsin missorting and constitutive activation in a transgenic rat model of retinitis pigmentosa. *Invest Ophthalmol Vis Sci* 2000;41:1546–1553. [PubMed: 10798675]
46. Sung CH, Makino C, Baylor D, Nathans J. A rhodopsin gene mutation responsible for autosomal dominant retinitis pigmentosa results in a protein that is defective in localization to the photoreceptor outer segment. *J Neurosci* 1994;14:5818–5833. [PubMed: 7523628]
47. Boesze-Battaglia K, Lamba OP, Napoli AA Jr, Sinha S, Guo Y. Fusion between retinal rod outer segment membranes and model membranes: a role for photoreceptor peripherin/rds. *Biochemistry* 1998;37:9477–9487. [PubMed: 9649331]
48. Luo W, Marsh-Armstrong N, Rattner A, Nathans J. An outer segment localization signal at the C terminus of the photoreceptor-specific retinol dehydrogenase. *J Neurosci* 2004;24:2623–2632. [PubMed: 15028754]
49. Helms JB, Zurzolo C. Lipids as targeting signals: lipid rafts and intracellular trafficking. *Traffic* 2004;5:247–254. [PubMed: 15030566]
50. Sandoval IV, Bakke O. Targeting of membrane proteins to endosomes and lysosomes. *Trends Cell Biol* 1994;4:292–297. [PubMed: 14731593]
51. Trowbridge IS, Collawn JF, Hopkins CR. Signal-dependent membrane protein trafficking in the endocytic pathway. *Annu Rev Cell Biol* 1993;9:129–161. [PubMed: 8280459]



Figure 1. Immunogold labeling of developing and rat photoreceptors with anti-peripherin/*rds* antibody Per3B6 (**A–E**) or anti-rhodopsin antibody, Rho4D2 (**F**). (**A**) At P5, peripherin/*rds* was detected at the distal end of the connecting cilium (cc, *arrowheads*) IS, inner segment. (**B**) At P6, outer segment membranes began accumulating at the distal connecting cilium and were heavily labeled with peripherin/*rds* antibody (*arrowhead*). (**C**) As outer segment discs organized in P8 photoreceptors, peripherin/*rds* was detected at various concentrations within the outer segment membranes. Distal membranes were more heavily labeled (*arrowhead*), whereas aligning discs specifically labeled putative rim regions (*arrow*). (**D**) At P15, peripherin/*rds* was localized to the rim region of outer segment discs (*arrowheads*) and to the region of the connecting cilium extending into the outer segment (*arrow*). (**E**) P5 photoreceptor inner segment (IS), showing that anti-peripherin/*rds* labeling was absent from inner segment membranes. (**F**) P5 photoreceptor labeled with anti-rhodopsin antibody, Rho4D2, showing significant labeling in the inner segment. Scale bars, 200 nm.

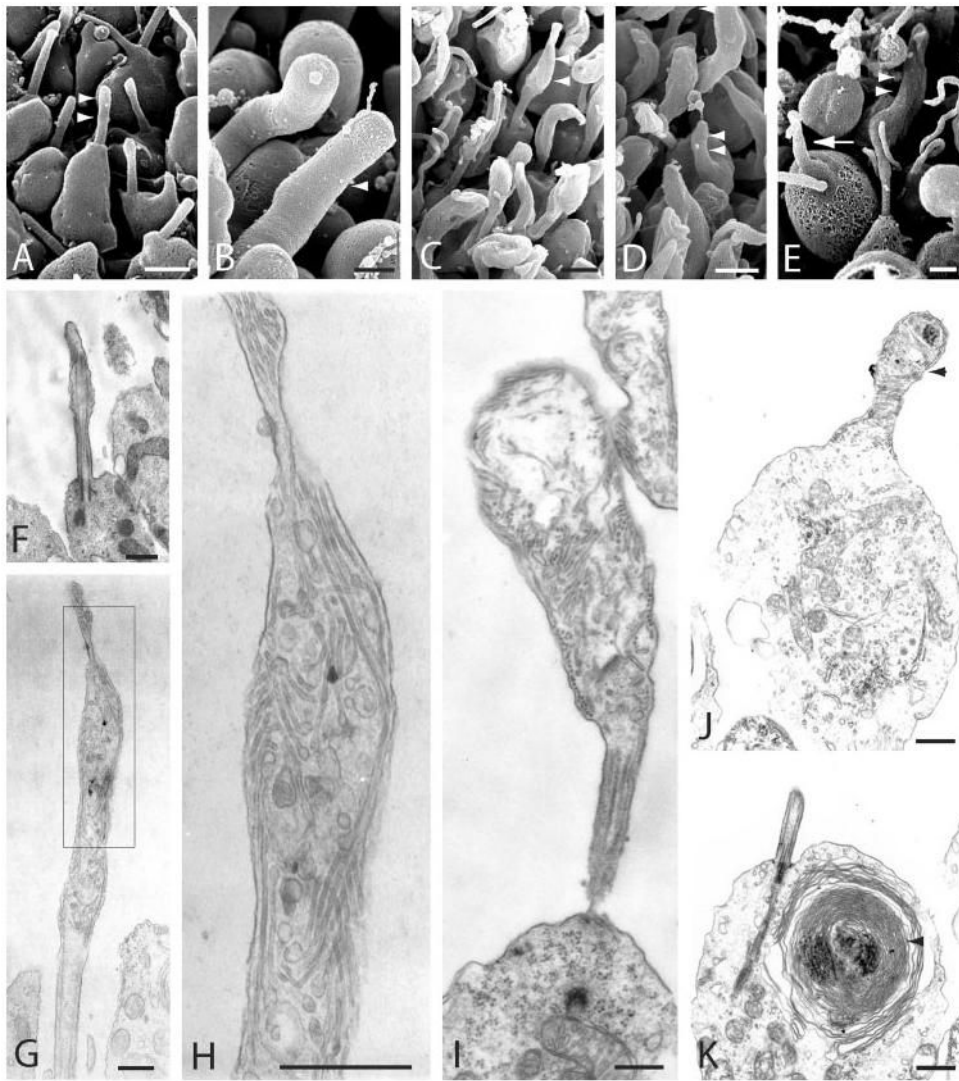


Figure 2. Rhodopsin-knockout photoreceptors created a rudimentary outer segment domain. (A–E) Scanning electron micrographs of the outer segment region in rhodopsin-knockout (A, C–E) and wild-type (B) mice. (A) P7 rhodopsin-knockout mice failed to recruit membranes to the distal connecting cilium (arrowheads). (B) Large outer segments (arrowhead) formed in P30 wild-type mouse photoreceptors. (C) At P30, small rudimentary outer segment domain membranes (arrowheads) projected from the connecting cilium in rhodopsin-knockout animals. (D) A tower-like protrusion (arrowheads) budded from the apical inner segment membrane in a P30 photoreceptor. (E) At P45, a few remaining outer segments were expanded in size (arrowheads), whereas other photoreceptors lacked outer segment membranes altogether (arrow). Many photoreceptors at this age were in various stages of degeneration. (F–K) Transmission electron micrographs of the outer segment domain membranes in rhodopsin-knockout mice. (F) The connecting cilium of P7 mice lacked membrane accumulation at the distal tip of the cilium, but otherwise developed normally. (G) The outer segment domain of P30-knockout mice consisted of various disorganized internal membranes surrounded by an external membrane. (H) A higher-magnification image of (B) showed internal membranes have tubular and/or vesicular profiles. (I) At P45, some remaining

photoreceptors formed larger outer segment domains. **(J)** An abnormal cell from a P45 retina with a fragmented inner segment membrane, fused mitochondria, and a membrane projection (*arrowhead*) budding from the apical inner segment. **(K)** On occasion, internal membranes (*arrowhead*) accumulated around a dense core within the inner segments of P45 photoreceptors. Scale bars: **(A–E)** 1 μm ; **(F–K)** 500 nm.

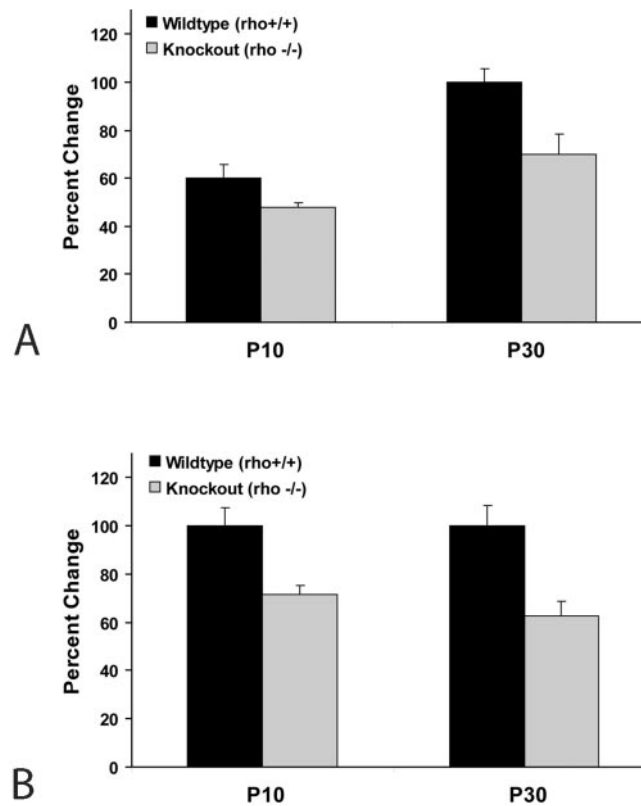


Figure 3. Peripherin/*rd5* and rom-1 expression in photoreceptors of rhodopsin-knockout mice. Transcripts of peripherin/*rd5* and rom-1 isolated from retinal extracts of P10 and P30 wild-type (rho^{+/+}) and rhodopsin-knockout (rho^{-/-}) mice were amplified using real-time RT-PCR. Gene expression was normalized to Thy-1 and percentage changes in expression were calculated relative to a WT P30 mouse (calibrator). At both ages examined, rhodopsin-knockout animals continued to transcribe moderate to moderately high levels of peripherin/*rd5* (A) and rom-1 (B), although expression levels were lower than the age-matched wild-type control. Results are expressed as the mean \pm SD of three animals per genotype per age.

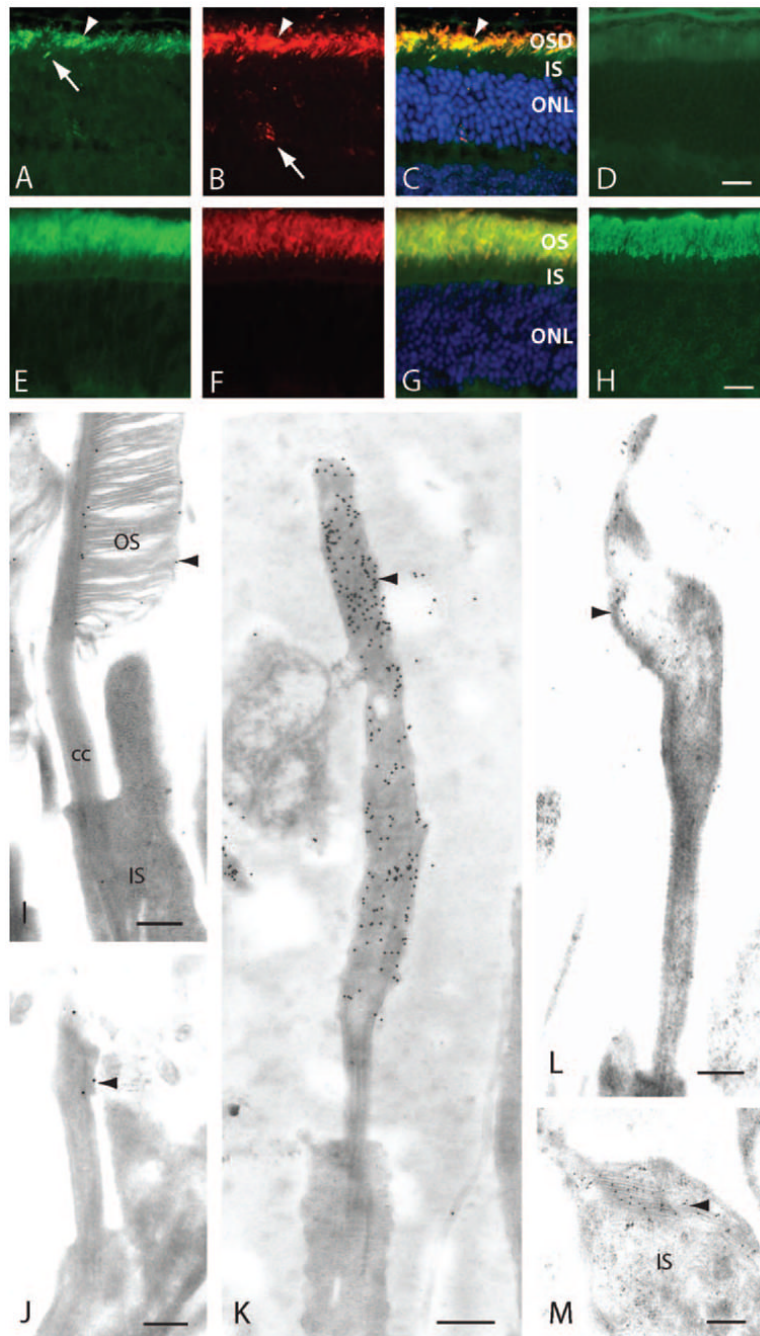


Figure 4.

Rim proteins peripherin/*rds* and rom-1 were transported to the outer segment domain (OSD) in the absence of rhodopsin. (A–D) Frozen sections of P30 rhodopsin-knockout retinas labeled with anti-peripherin/*rds*, Mper5H2 (A), anti-rom-1 C-1 (B), and anti-rhodopsin Rho4D2 (D). (A) Peripherin/*rds* localized to the OSD membranes (arrowhead) in rhodopsin-knockout photoreceptors. Inner segment (IS) and photoreceptor nuclei did not label except for one possible cell with IS mislocalization (arrow) (B) Rom-1 also distributed to the OSD (arrowhead) in rhodopsin-knockout rod photoreceptors. On occasion, delocalized rom-1 was detected in the outer nuclear layer (ONL, arrow). (C) Merged image of (A) and (B) plus Hoechst 33342 nuclear dye, showing colocalization of rom-1 with peripherin/*rds* in the OSD

(*arrowhead*). (**D**) Only nonspecific RPE background and OS autofluorescence were detected in sections probed with anti-rhodopsin antibody. (**E–H**) Wild-type mice immunostained with antibodies against peripherin/*rds* (**E**), rom-1 (**F**), and rhodopsin (**H**). (**G**) Merged image of (**E**) and (**F**) with Hoechst 33342 nuclear dye showing labeling of rim proteins restricted to the OS. (**H**) Anti-rhodopsin antibody labeling photoreceptor OS. (**I–M**) Electron micrographs of wild-type (**I**) and rhodopsin-knockout mice (**J–M**) immunogold labeled with anti-peripherin/*rds* and anti-rom-1 antibodies. (**I**) Anti-rom-1 C-1 antibody labeled disc rims (*arrowhead*) specifically in wild-type mice photoreceptors. (**J**) In developing P7 photoreceptors of rhodopsin-knockout rods, rom-1 localized exclusively to the distal connecting cilium (cc, *arrowhead*). (**K**) Older P30 photoreceptors accumulated rom-1 throughout the OSD membranes (*arrowheads*) which budded from the tip of the connecting cilium. Rom-1 was not detectable in the IS membranes or cytoplasm. (**L**) Peripherin/*rds* was also present in the OSD membranes (*arrowhead*). (**M**) Anti-rom-1 antibody labeled ectopic membranes (*arrowhead*) that accumulated within the IS of a small fraction of cells. Scale bars: (**A–D**) 10 μm ; (**E–H**) 15 μm ; (**I–M**) 250 nm.

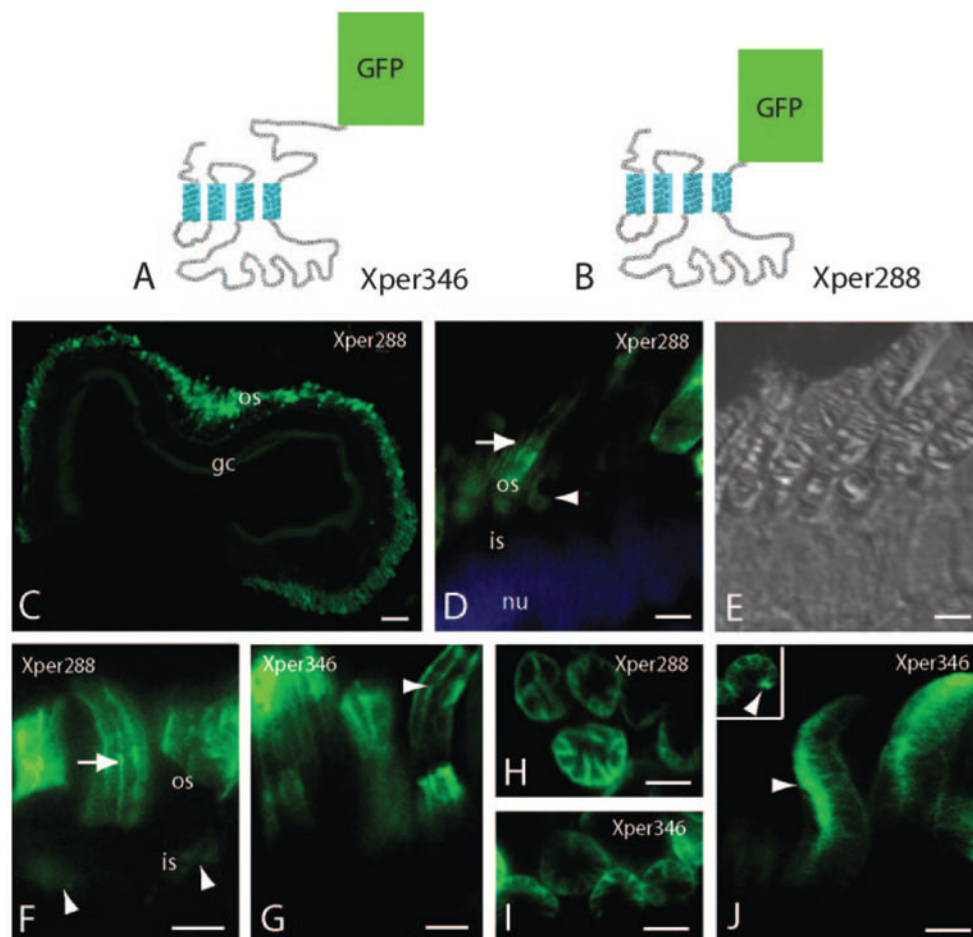


Figure 5.

Transport of C-terminally truncated peripherin/*rds* in transgenic *Xenopus laevis* photoreceptors. (A, B) Diagram of *Xenopus* peripherin/*rds*, Xper38, fusion proteins. (A) GFP is attached to the C terminus of full-length peripherin/*rds* to create Xper346. (B) A C-terminally truncated peripherin/*rds* with its last 58 amino acids removed is fused with GFP to generate Xper288. (C) Expression of the C-terminally truncated peripherin/*rds*-GFP fusion protein (Xper288) in the retina of transgenic *Xenopus laevis* was restricted to photoreceptors. (D, F) Xper288 fusion protein was predominantly localized to the outer segment (OS) of rods (arrow) and cones (arrowhead in D). Blue: DAPI stain of nuclei. (E) Brightfield DIC image of the retina from (D). (F) In an occasional photoreceptor, low levels of fusion protein Xper288 delocalized to the inner segment. Xper288 fusion protein was faintly detected in the inner segment (arrowheads) of photoreceptors neighboring a rod cell with only disc rim and incisure localization (arrow). Incisures fluoresced as vertical striations. (G) Full-length peripherin/*rds*-GFP (Xper346) localized to the outer segment and was not detected in the inner segment. (H, I) Transverse cross section of outer segments showing both Xper288 (H) and Xper346 (I) localization to disc rims and incisures. (J) A photoreceptor expressing high levels of Xper346 was visualized, having peripherin/*rds*-GFP accumulation as a vertical column (arrowhead) within the outer segment. Inset: Transverse cross section of an outer segment showing fusion protein accumulation (arrowhead). GFP, green fluorescent protein; os, outer segment; gc, ganglion cell; is, inner segment; nu, nucleus. Scale bars: (C) 100 μm ; (D–J) 5 μm .

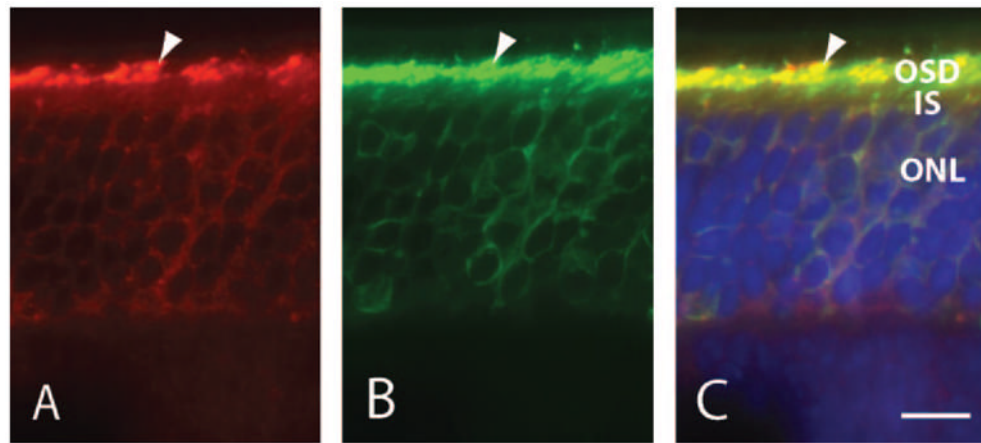


Figure 6.

Distribution of rom-1 and rhodopsin in *rds* photoreceptors. Frozen sections of P23 *rds* mice retinas were labeled with anti-rom-1 C-1 (*red*), anti-rhodopsin, Rho4D2 (*green*), and Hoechst 33342 nuclear dye (*blue*). (A) Rom-1 localized predominantly to the outer segment domain (*arrowhead*) while delocalizing to a lesser extent to the inner segment, cell body, and synaptic terminals of rod photoreceptors. (B) Rhodopsin also accumulated in the outer segment domain (*arrowhead*) and was present in lower levels in the inner segment, cell body, and synaptic terminal. (C) Rom-1 and rhodopsin colocalized predominantly within the outer segment domain (*arrowhead*). OSD, outer segment domain; IS, inner segment; ONL, outer nuclear layer. Scale bar, 10 μm .